DNA Nanostructures

DOI: 10.1002/anie.201403236

# Single-Particle Tracking and Modulation of Cell Entry Pathways of a Tetrahedral DNA Nanostructure in Live Cells**

*Le Liang, Jiang Li, Qian Li, Qing Huang,* Jiye Shi, Hao Yan, and Chunhai Fan**

***Abstract:*** *DNA is typically impermeable to the plasma membrane due to its polyanionic nature. Interestingly, several different DNA nanostructures can be readily taken up by cells in the absence of transfection agents, which suggests new opportunities for constructing intelligent cargo delivery systems from these biocompatible, nonviral DNA nanocarriers. However, the underlying mechanism of entry of the DNA nanostructures into the cells remains unknown. Herein, we investigated the endocytotic internalization and subsequent transport of tetrahedral DNA nanostructures (TDNs) by mammalian cells through single-particle tracking. We found that the TDNs were rapidly internalized by a caveolin-dependent pathway. After endocytosis, the TDNs were transported to the lysosomes in a highly ordered, microtubule-dependent manner. Although the TDNs retained their structural integrity within cells over long time periods, their localization in the lysosomes precludes their use as effective delivery agents. To modulate the cellular fate of the TDNs, we functionalized them with nuclear localization signals that directed their escape from the lysosomes and entry into the cellular nuclei. This study improves our understanding of the entry into cells and transport pathways of DNA nanostructures, and the results can be used as a basis for designing DNA-nanostructure-based drug delivery nanocarriers for targeted therapy.*

The use of DNA as a material has become commonplace, especially with the emergence of DNA nanotechnology.[1] A large number of well-defined DNA nanostructures of varying dimensions, shapes, and geometries have been assembled by exploiting the highly specific and programmable nature of DNA base pairing.[2–6] Among the many potential uses of DNA nanostructures, biological and biomedical applications are very attractive because of the biological nature of DNA. DNA nanostructures typically exhibit low cytotoxicity and are highly resistant to enzymatic degradation in biological media, which are favorable properties for in vivo applications.[7–10] Recently, tetrahedral DNA nanostructures (TDNs) were shown to be permeable to the cellular membrane, a property distinct from that of their linear counterparts (single- and double-stranded DNA; ssDNA and dsDNA, respectively). This discovery advocates new opportunities for DNA-based bioimaging and smart drug delivery into live cells and small animals.[8,11–15] Nevertheless, the mechanism for agent-free internalization of DNA nanostructures remains largely unexplored.

Cellular uptake of DNA typically relies on positively charged transfection agents that, together with the DNA, form charge-compensated complexes, which allows the DNA to traverse the negatively charged cellular membrane. Interestingly, despite their net negative charge, DNA nanostructures can be internalized by mammalian cells without the aid of transfection agents.[7,8] Intuitively, we surmised that cellular internalization of these structurally well-defined nano-objects was mediated by very specific endocytotic pathways. Thus, we sought to interrogate the dynamic interactions between DNA nanostructures and their cellular hosts in an effort to better understand the nanostructure uptake and to subsequently design an improved class of DNA-nanostructure-based delivery vehicles. In addition, this study may provide new insight into the mechanisms of viral infection, due to the striking structural similarities between DNA nanostructures and virus particles, especially capsid-free viroids and the hepatitis Delta virus.[16,17] In this work, we utilized single-particle tracking to monitor the entry and transport pathways of TDNs in live cells. We also developed a strategy to modulate the intracellular fate of the TDNs for targeted delivery of a cargo.

The TDNs were self-assembled from four 55-base ssDNA strands (Table S1 in the Supporting Information) with rationally designed, partially complementary sequences (Figure S1 A in the Supporting Information).[18,19] The successful formation of the TDNs ($\approx 90\%$ yield) was confirmed by polyacrylamide gel electrophoresis (PAGE) and atomic force microscopy (AFM; Figure S1B and C in the Supporting Information). We labeled each vertex of the TDNs with cyanine-3 (Cy3) fluorophores (Cy3-TDNs) to facilitate single-particle tracking monitored by fluorescence microscopy (Figure S1 A in the Supporting Information).

[*] L. Liang, Dr. J. Li, Dr. Q. Li, Prof. Q. Huang, Dr. J. Shi, Prof. C. Fan
Division of Physical Biology, and Bioimaging Center, Shanghai Synchrotron Radiation Facility, CAS Key Laboratory of Interfacial Physics and Technology, Shanghai Institute of Applied Physics
Chinese Academy of Sciences, Shanghai 201800 (China)
E-mail: huangqing@sinap.ac.cn
fchh@sinap.ac.cn
Homepage: http://www.sinap.ac.cn/physbio/faculty/Chunhai_Fan.htm

Prof. H. Yan
Center for Molecular Design and Biomimicry, Biodesign Institute, Department of Chemistry and Biochemistry
Arizona State University, Tempe, AZ 85287 (USA)

Dr. J. Shi
UCB Pharma, Slough SL1 3WE (UK)

[**] This work was supported by the Ministry of Science and Technology of China (2013CB933802, 2012CB825805, 2013CB932803), the National Science Foundation of China (21390414, 21227804, 91313302), and the Chinese Academy of Sciences.

Supporting information for this article is available on the WWW under http://dx.doi.org/10.1002/anie.201403236.

  

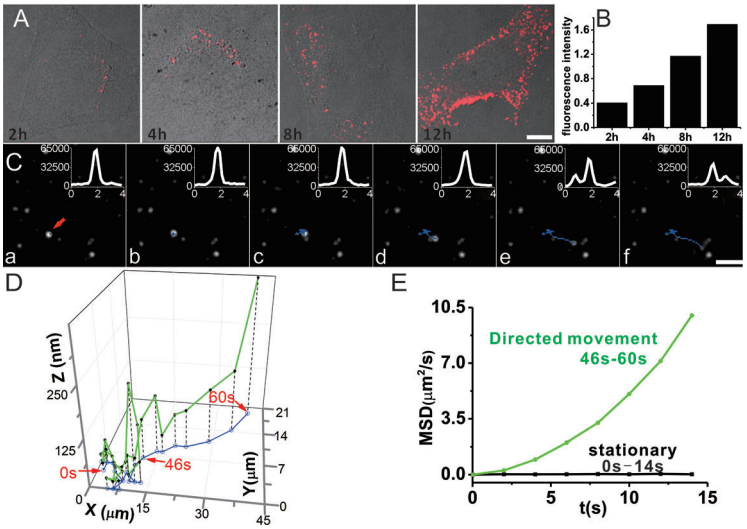


***Figure 1.*** Internalization of TDNs by HeLa cells. A) Confocal images of HeLa cells treated with Cy3-TDNs for 2, 4, 8, and 12 h. Scale bar: 10 μm. B) Flow cytometry analysis of cellular uptake of Cy3-TDNs. C) Uptake of a single TDN by a HeLa cell visualized with a TIRF microscope. Selected frames (a–f) show internalization of the TDN particle in real time (see also Video 1 in the Supporting Information). The blue line indicates the trajectory (projected in the *X*–*Y* plane) of a selected TDN. The decrease and disappearance of fluorescence indicates that the particle is moving away from the surface of the slide and is being taken up by the cell. Scale bar: 5 μm. D) 3D trajectory of the TDN shown in (C). The fluorescence intensity is converted into distance in the *Z* direction. The blue line corresponds to the *X*–*Y* trajectory, as shown in (C), and the green line maps the 3D trajectory. E) 3D mean square displacement (MSD) analysis of TDN movement. The trajectory follows two phases: the TDN remains static on the slide surface for at least 45 s and then moves rapidly along the *z* axis.

We incubated HeLa cells with Cy3-labeled TDNs at 37 °C and continuously monitored the internalization process over 12 h by confocal microscopy and flow cytometry (Figure 1 A and B). Both analysis methods revealed the evolution of cellular uptake of Cy3-TDNs over time; that is, the fluorescence intensity increased over time until the cytoplasm was saturated by red fluorescence at 12 h. It is noteworthy that the internalized TDNs remained intact inside the cells for at least 8 h, as revealed in our previous Förster resonance energy transfer (FRET) study.[8] We also note that the Cy3-TDNs did not enter the nucleus, as shown by fluorescence monitoring.

The real-time transmembrane kinetics of the TDNs were monitored by total internal reflection fluorescence (TIRF) microscopy (Figure 1 C). TIRF microscopy is a powerful tool to study intracellular particles because of its low background interference, high sensitivity, and high resolution. We monitored a single Cy3-TDN particle by using TIRF microscopy, as shown in Figure 1 C a. This particle must be within 300 nm of the surface because it is visible in the TIRF images. The fluorescence is expected to decrease exponentially as the particle moves farther away from the surface in the *Z* direction and to disappear when the particle is more than 300 nm from the surface.[20] We observed two distinct phases of motion of the Cy3-TDN. In the first phase, the Cy3-TDN particle was stationary and emitted bright fluorescence for at least 45 s (the observation timescale of TIRF microscopy). In the second phase, the particle spot moved quickly and the fluorescence rapidly decreased to an undetectable level within 15 s. We did not observe significant photobleaching of the Cy3-TDN over 60 s, which corresponds to the period of image acquisition (Figure 1 C and Video S1 in the Supporting Information). Thus, the sharp change in fluorescence emission that we observed is an indication of motion of the Cy3-TDN particle in the *Z* direction. Mean square displacement (MSD) analysis of the tracking data provides further evidence of this motion. Three-dimensional trajectory analysis for the Cy3-TDN particle confirms the presence of two phases (Figure 1 D and E). The first phase ($>45$ s long) can be attributed to random movement of the membrane-bound Cy3-TDN; the particle remains close to the surface ($<300$ nm), so we observe strong fluorescence. The second phase ($\approx 15$ s long) is attributed to internalization of the Cy3-TDN, which is a very rapid process that results in the delivery of the particle into the cytoplasm. The internalized Cy3-TDN escapes from the excitable region of TIRF microscopy due to the micron scale of cells; consequently, the fluorescent emission from the particle disappears over time.

Having established cellular entry of TDNs at the single-particle level, we further investigated the entry pathway through a set of cell biological and fluorescence imaging experiments. We first studied the membrane–TDN fusion process by performing colocalization experiments with two-color confocal microcopy (Figure 2 A and Video S2 in the Supporting Information). The lipid bilayer of the cellular membrane was stained with a green-emitting lipophilic dye (DiO).[21] We observed colocalization of the fluorescence from Cy3 (red) and DiO (green), as well as a corresponding fluorescence increase in a synchronized manner, which suggests that the TDNs fused with the membrane and were probably buried in DiO-labeled lipid pits.[21] The fusion process occurred over approximately 87 s, which is in agreement with the single-particle tracking data (Figure 2 B). These results complement our previous functional studies with cytosine–phosphodiester–guanine (CpG)-modified TDNs.[8] In that report, we determined that CpG-TDNs trigger immunostimulatory activity in mammalian immune cells by binding to Toll-like receptor 9 (TLR9) in the endosomal membrane.[22] TDNs are negatively charged particles, so it is highly unlike that they enter cells by passive processes because of the electrostatic repulsion. Taken together, the results indicate that the TDNs fuse with the cellular membrane and subsequently enter the endosomes through endocytosis.

We also studied the energy dependence of the cellular uptake through a temperature experiment. At 4 °C, all active energy-dependent endocytotic processes are stalled.[23] Therefore, we incubated Cy3-TDNs with HeLa cells at 4 and 37 °C and determined the position of the particles by 3D optical sectioning. By reconstructing 3D images of single cells, we were able to accurately identify the location of the TDNs within the cells (Figure 2 C and D). Interestingly, we observed

  

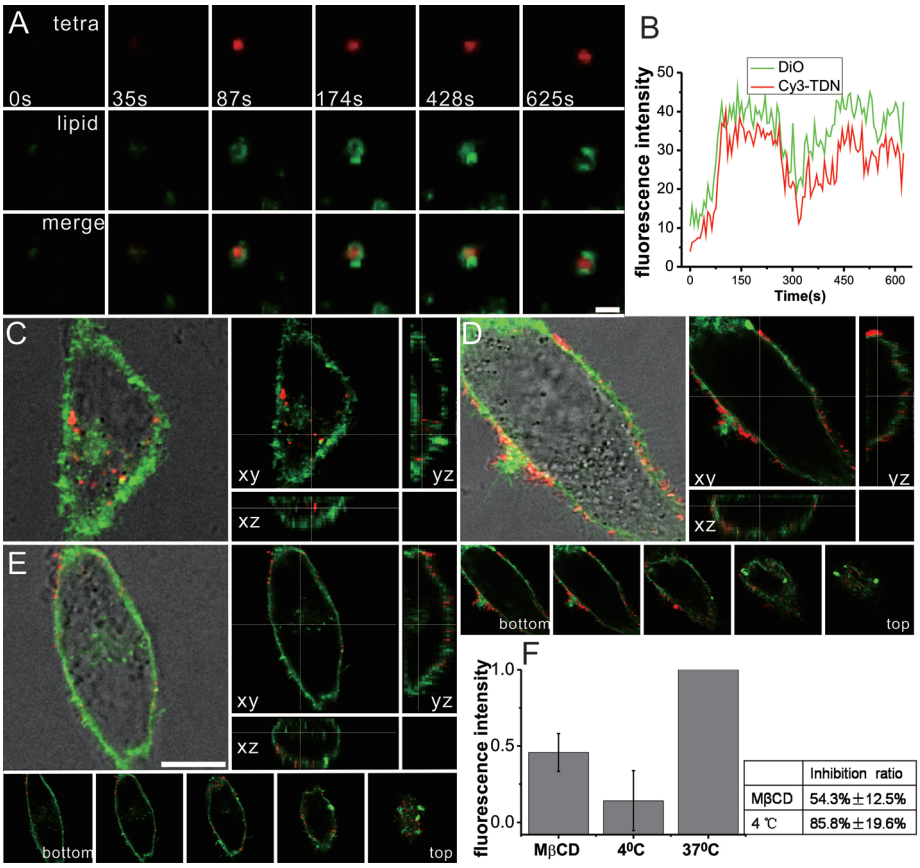


***Figure 2.*** Receptor-mediated endocytosis of TDNs in HeLa cells. A) Confocal images of an internalized Cy3-TDN particle (red) at different time points, colocalized with DiO-labeled lipid (green). Scale bar: 1 μm. (See also Video 2 in the Supporting Information.) B) Evolution of the fluorescence of the Cy3-TDN (red) and DiO-labeled lipid (green) particles selected in (A) over time. Reconstructed 3D images of a DiO-stained HeLa cell incubated with Cy3-TDNs for 6 h C) at 37 °C without methyl-β-cyclodextrin (MβCD), D) at 4 °C without MβCD, and E) at 37 °C and pretreated for 30 min with 10 mM MβCD. Scale bar: 10 μm. F) Fluorescence intensity of internalized TDNs by cells pretreated with MβCD or incubated at 4 °C or 37 °C. Data were obtained by flow cytometry analysis.

a dramatic reduction in the cellular uptake of the TDNs at 4 °C. Relative to the results of the experiments performed at 37 °C, Cy3 emission decreased by (85.8 ± 19.6) % at 4 °C (Figure 2F), which suggests that endocytosis of TDNs is energy dependent. We also note that the residual fluorescence observed at 4 °C may be a result of adsorption of Cy3-TDNs on the cellular membrane, as evidenced in the optical sectioning images (Figure 2D). In addition, we conclude that TDN uptake is a receptor-mediated process because the addition of cytochalasin D, an inhibitor for non-receptor-mediated endocytosis,[24] did not lead to an obvious decrease in fluorescence.

Next, we sought to identify the particular endocytotic pathway of the TDNs into the cells. Clathrin-dependent and caveolin-dependent pathways are the two major receptor-mediated endocytotic processes.[25] To evaluate the roles of these processes in the endocytosis of TDNs, we separately employed inhibitors to selectively block one of the two pathways. Treatment of HeLa cells with methyl-β-cyclodextrin (MβCD), which depletes cholesterol and disrupts caveolae and, thus, caveolin-dependent endocytosis,[26] greatly reduced (by (54.3 ± 12.5) %) the uptake of Cy3-TDNs, as evidenced by the observed decrease in fluorescence in the flow cytometry data (Figure 2E and F). It is important to note that the residual fluorescence observed in the flow cytometry data arises from Cy3-TDN adsorption on the membranes, rather than entry of Cy3-TDNs into the cells, because the corresponding fluorescent spots are primarily distributed on the membrane, as observed in optical sectioning (Figure 2D and E). In contrast, treatment of the cells with sucrose, an inhibitor for the clathrin-mediated pathway,[27] did not reduce the uptake of Cy3-TDNs (Figure S2 in the Supporting Information). To further substantiate that endocytosis of TDNs is caveolin dependent, we interrogated the entry of TDNs in a different cell line, COS-7, which showed similar results (Figure S3 in the Supporting Information).

Beyond the cellular uptake of TDNs, we were also interested in determining the fate of TDNs inside the cells. We studied the intracellular transport of TDNs through live cell imaging. Cy3-TDNs were incubated with HeLa cells, and the motion of individual fluorescently labeled particles was tracked in real time. As shown in Figure 3A (and Video S3 in the Supporting Information), the majority of TDN particles entered the cells within 6 h and subsequently exhibited high motility inside the cells. We generated a maximum time projection from the time-lapse movies that were acquired, which provides visualization of the trace and range of motion by recording pixels with maximum fluorescence intensity from each frame and integrating them into a single picture.[28] By using this method, we observed the transport of Cy3-TDNs within the entire area of a single live cell. The motion of the TDNs that we observed can be divided into two types: very rapid and static. To quantify these, we randomly selected 100 TDN particles in a single cell and analyzed their intracellular trajectories. We observed that approximately 60 % of the TDN particles were confined to a small area and exhibited very little movement (example indicated by the red arrow in Figure 3D), whereas other TDN particles moved rapidly with an average speed of 0.25 $\mu m s^{-1}$ (example indicated by the black arrow in Figure 3D).

We went on to investigate the mechanism of intracellular motion of the TDNs. Colocalization experiments revealed that the red fluorescence of Cy3-TDNs largely overlapped

  

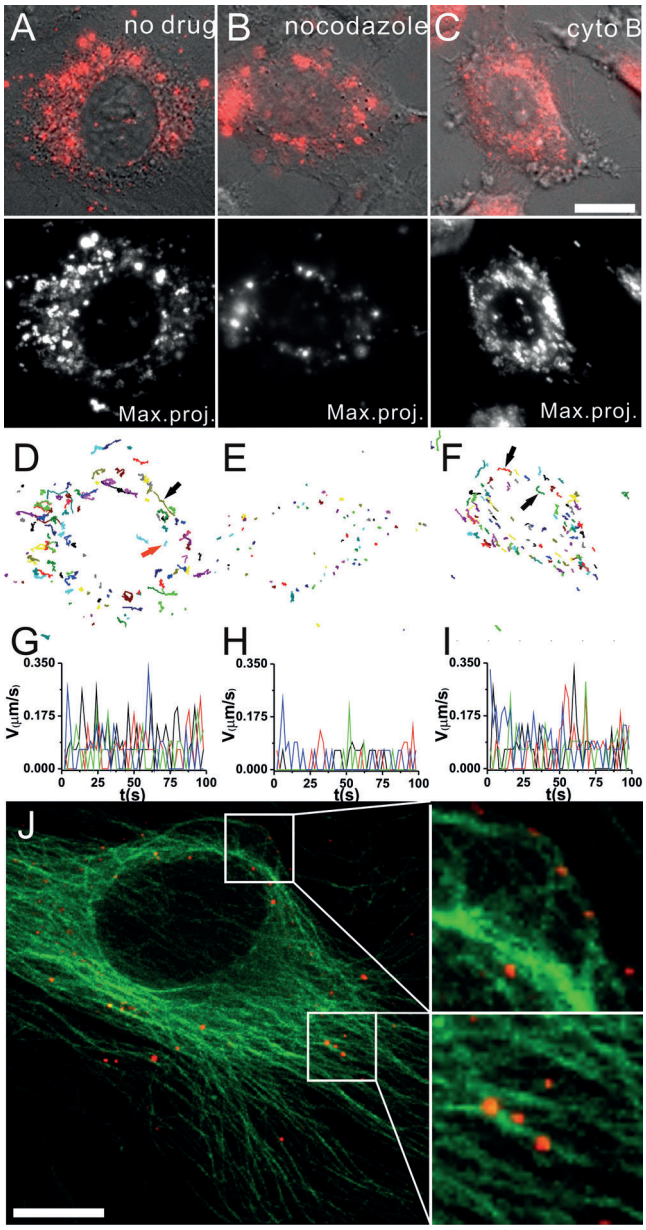


***Figure 3.*** A–C) Confocal images of HeLa cells incubated with Cy3-TDNs (red). Max.proj.: maximum time projection. D–F) Representative trajectories of 100 randomly selected TDN particles (see also Video 3, 4, and 5 in the Supporting Information). G–I) Speed of TDNs in untreated cells or cells pretreated with 60 μM nocodazole or 10 μM cytochalasin for 30 min. The black and red arrows in (D) indicate fast- and slow-moving particles in a confined area, respectively. Successive points in the trajectories are separated by 2 s. Scale bars of confocal images: 10 μm. J) Confocal images of TDNs (red) colocalized with microtubulin (green) in HeLa cells. Scale bar: 10 μm.

with the green fluorophore-stained microtubules (Figure 3J), which suggested microtubule-dependent transport of the TDNs. To probe this further, we separately employed inhibitors of either microtubules or actins to selectively block one of the two pathways. In cells pretreated with nocodazole, which depolymerizes tubulins,[21] the TDNs were confined to a small area and their movement was dramatically reduced to an average speed of $< 0.1\ \mu m\,s^{-1}$ (Figure 3B, E, and H and Video S4 in the Supporting Information). In contrast, the motility of the TDNs remained largely the same in cells pretreated with cytochalasin B, a chemical that completely depolymerizes actins[21] (Figure 3C, F, and I and Video S5 in the Supporting Information). Taken together, these results indicate that the intracellular motility of DNA tetrahedra is dependent on microtubules and independent of actin microfilaments.

We observed that a substantial portion of the TDNs were confined to a small area in the HeLa cells, with no mobility after 6 h of incubation, so we suspected that the particles had been delivered to specific locations. To establish this, we prolonged the incubation time to 12 h and subsequently performed colocalization experiments. We stained the cells with lysotracker, a green fluorophore that binds specifically to lysosomes. Interestingly, we observed yellow areas in the confocal images, which were the result of overlapping red fluorescence from the Cy3-TDNs and green fluorescence from the labeled lysosomes; this result suggests that the TDNs were localized to the lysosomes (Figure S4 in the Supporting Information). Time-evolution studies showed that internalized TDNs reached the lysosomes in approximately 3 h and localization of the TDNs increased along with incubation time. Cellular optical sectioning (from bottom to top) further revealed that most internalized TDNs were confined to the lysosomes after 6 h incubation (Figure S4B in the Supporting Information). We performed quantitative analysis on 10 randomly selected cells and found that approximately 70–80% of the TDNs were localized in the lysosomes (Figure S4 in the Supporting Information).

Having established that internalized TDNs are eventually delivered to the lysosomes, we sought to modulate the fate of the TDNs inside the cells with the hope that cell-permeable TDNs could eventually be used as nanocarriers for cellular cargo. We functionalized the TDNs with nucleus-targeting signaling peptides that display nuclear localization signals (NLSs)[29] through a "click" reaction, which efficiently couples azide-modified ssDNAs to NLS peptides containing a propargylglycine (Figure S7A and B in the Supporting Information). To visualize the NLS-TDNs in HeLa cells, we labeled the NLSs with TAMRA (red) and the TDNs with Alexa 488 (green). HeLa cells were incubated with NLS-TDNs for 16 h and subsequently stained with Hochest 33342 (blue), a nucleus staining dye (Figure 4). The NLS-TDNs remained intact in the cell, as evidenced by the spatial colocalization of the red and green fluorescence. Significantly, optical sectioning demonstrated that the NLS-TDNs were localized within the nucleus, whereas TDNs without NLSs were mostly restricted to the cytoplasm. Thus, we conclude that the attachment of NLSs to the TDN particles modulates their cellular fate, which would otherwise restrict them to the lysosomes.

The plasma membrane is the first boundary between external particles and cells. Direct transport of DNA molecules across the plasma membrane is generally not feasible due to their large size and highly negative charge. Remarkably, recent findings showed that structured DNA is efficiently internalized by cells; thus, DNA nanostructures hold great promise for biomedical applications.[7–10] With rapid

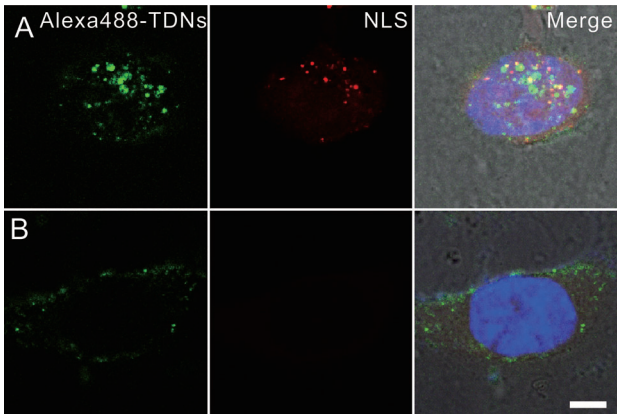


***Figure 4.*** Confocal images of HeLa cells treated with Alexa 488-labeled TDNs (green) A) with or B) without NLS functionalization (red). The nucleus was stained with Hoechst 33342 (blue). Scale bar: 10 μm.

advances in DNA nanotechnology, it is now practical to design and fabricate DNA nanostructures with tailored sizes, shapes, and geometries.[2–6] Studies of their ability to penetrate cellular membranes and the pathways with which they enter cells may provide new clues about the mechanisms of viral infection (because of the structural similarities between some DNA nanostructures and viral particles) and may aid in the development of new tools for bioengineering, including nonviral transfection methods and gene therapy. Based on the studies described above, we created a summary of our findings on the cellular entry, transport, and fate of TDNs, as presented in Figure S6 in the Supporting Information.

In typical energy-dependent endocytosis, small particles (< 500 nm) first bind nonspecifically to the plasma membrane and are then internalized through mediation by receptors.[30] The type of endocytotic pathway that is employed is critically dependent on the size of the endocytotic vesicles. Previous studies on viral entry by endocytosis suggest that caveolae vesicles are 50–60 nm in diameter and can only carry very small particles,[31,32] such as the 7 nm TDNs employed in this study.

The cytoplasm is a highly crowded environment with a densely packed network of organelles, macromolecules, and cytoskeletal elements. Hence, it is unlikely that internalized TDN particles freely diffuse in the cytoplasm after endocytosis.[33] Both colocalization and inhibition studies revealed that their transport is microtubule dependent and actin filament independent. That is, the TDNs are transported in a highly ordered manner with the help of molecular motors (kinesin and dynein).[34,35] It is also worthwhile to note that the TDNs retain their structural integrity during this microtubule-dependent transport, as evidenced by previous FRET-based analysis.[9] The stability of the TDNs stems from their resistance to nuclease attack, which makes them promising as nanoscale carriers for nonviral drug delivery.

Despite these attractive features, we discovered that most TDNs are transported to, and trapped within, the lysosomes. Lysosomes are organelles in which invading particles are digested, so it is apparent that TDNs are regarded as foreign substances rather than inherent genetic materials. Although our previous studies showed that TDNs effectively display CpG oligonucleotides to stimulate the immune response of macrophage cells, they actually function inside the lysosome by binding to TLR9.[8] Thus, it would be difficult to develop DNA-nanostructure-based drug delivery modules if lysosome degradation is their ultimate fate. To address this problem, we further demonstrated that TDNs could be directed to specific organelles (in this case, the nucleus) by displaying the appropriate modifications, such as signaling peptides. This advance opens new opportunities for targeted therapies, including regulation of replication and transcription.

Received: March 11, 2014
Published online: May 14, 2014

**Keywords:** cell internalization · cell transport · DNA structures · nanostructures · single-particle tracking

[1] N. C. Seeman, *Nature* **2003**, *421*, 427.
[2] H. Dietz, S. M. Douglas, W. M. Shih, *Science* **2009**, *325*, 725.
[3] T. Liedl, B. Hogberg, J. Tytell, D. E. Ingber, W. M. Shih, *Nat. Nanotechnol.* **2010**, *5*, 520.
[4] D. Han, S. Pal, J. Nangreave, Z. Deng, Y. Liu, H. Yan, *Science* **2011**, *332*, 342.
[5] P. W. K. Rothemund, *Nature* **2006**, *440*, 297.
[6] Y. M. Fu, D. D. Zeng, J. Chao, Y. Q. Jin, Z. Zhang, H. J. Liu, D. Li, H. W. Ma, Q. Huang, K. V. Gothelf, C. H. Fan, *J. Am. Chem. Soc.* **2013**, *135*, 696.
[7] A. S. Walsh, H. Yin, C. M. Erben, M. J. A. Wood, A. J. Turberfield, *ACS Nano* **2011**, *5*, 5427.
[8] J. Li, H. Pei, B. Zhu, L. Liang, M. Wei, Y. He, N. Chen, D. Li, Q. Huang, C. Fan, *ACS Nano* **2011**, *5*, 8783.
[9] H. Pei, L. Liang, G. B. Yao, J. Li, Q. Huang, C. H. Fan, *Angew. Chem.* **2012**, *124*, 9154; *Angew. Chem. Int. Ed.* **2012**, *51*, 9020.
[10] S. Modi, M. G. Swetha, D. Goswami, G. D. Gupta, S. Mayor, Y. Krishnan, *Nat. Nanotechnol.* **2009**, *4*, 325.
[11] Y. Benenson, B. Gil, U. Ben-Dor, R. Adar, E. Shapiro, *Nature* **2004**, *429*, 423.
[12] S. Ko, H. Liu, Y. Chen, C. Mao, *Biomacromolecules* **2008**, *9*, 3039.
[13] H. Lee, A. K. R. Lytton-Jean, Y. Chen, K. T. Love, A. I. Park, E. D. Karagiannis, A. Sehgal, W. Querbes, C. S. Zurenko, M. Jayaraman, C. G. Peng, K. Charisse, A. Borodovsky, M. Manoharan, J. S. Donahoe, J. Truelove, M. Nahrendorf, R. Langer, D. G. Anderson, *Nat. Nanotechnol.* **2012**, *7*, 389.
[14] Q. Jiang, C. Song, J. Nangreave, X. Liu, L. Lin, D. Qiu, Z.-G. Wang, G. Zou, X. Liang, H. Yan, B. Ding, *J. Am. Chem. Soc.* **2012**, *134*, 13396.
[15] S. M. Douglas, I. Bachelet, G. M. Church, *Science* **2012**, *335*, 831.
[16] M. Lakadamyali, M. J. Rust, X. Zhuang, *Cell* **2006**, *124*, 997.
[17] C. Chen, X. Zhuang, *Proc. Natl. Acad. Sci. USA* **2008**, *105*, 11790.
[18] R. P. Goodman, R. M. Berry, A. J. Turberfield, *Chem. Commun.* **2004**, 1372.
[19] H. Pei, N. Lu, Y. Wen, S. Song, Y. Liu, H. Yan, C. Fan, *Adv. Mater.* **2010**, *22*, 4754.
[20] D. Axelrod, *Traffic* **2001**, *2*, 764.
[21] J. C. Vaughan, B. Brandenburg, J. M. Hogle, X. Zhuang, *Biophys. J.* **2009**, *97*, 1647.
[22] Y. Kumagai, O. Takeuchi, S. Akira, *Adv. Drug Delivery Rev.* **2008**, *60*, 795.
[23] N. W. S. Kam, Z. Liu, H. Dai, *Angew. Chem.* **2006**, *118*, 605; *Angew. Chem. Int. Ed.* **2006**, *45*, 591.
[24] J. Rejman, V. Oberle, I. S. Zuhorn, D. Hoekstra, *Biochem. J.* **2004**, *377*, 159.

  

[25] B. Brandenburg, X. Zhuang, *Nat. Rev. Microbiol.* **2007**, *5*, 197.
[26] M. G. Qaddoumi, H. J. Gukasyan, J. Davda, V. Labhasetwar, K. J. Kim, V. H. L. Lee, *Mol. Vision* **2003**, *9*, 559.
[27] J. E. Heuser, R. G. W. Anderson, *J. Cell Biol.* **1989**, *108*, 389.
[28] A. Mor, S. Suliman, R. Ben-Yishay, S. Yunger, Y. Brody, Y. Shav-Tal, *Nat. Cell Biol.* **2010**, *12*, 543.
[29] M. A. Zanta, P. Belguise-Valladier, J. P. Behr, *Proc. Natl. Acad. Sci. USA* **1999**, *96*, 91.
[30] J. A. Dix, A. S. Verkman, *Annu. Rev. Biophys.* **2008**, *37*, 247.
[31] T. Kirchhausen, *Annu. Rev. Biochem.* **2000**, *69*, 699.
[32] B. J. Nichols, J. Lippincott-Schwartz, *Trends Cell Biol.* **2001**, *11*, 406.
[33] J. A. Spudich, *Nature* **1994**, *372*, 515.
[34] R. D. Vale, R. A. Milligan, *Science* **2000**, *288*, 88.
[35] T. Soldati, M. Schliwa, *Nat. Rev. Mol. Cell Biol.* **2006**, *7*, 897.

  